Extra modes of operation and self motions in manipulators designed for Schoenflies motion

Michel Coste, Kartoue Mady Demdah

▶ **To cite this version:**

Michel Coste, Kartoue Mady Demdah. Extra modes of operation and self motions in manipulators designed for Schoenflies motion. Journal of Mechanisms and Robotics, 2015, 7 (4), pp.41020-41020. 10.1115/1.4029501 . hal-01056473

HAL Id: hal-01056473
https://hal.science/hal-01056473

Submitted on 20 Aug 2014

HAL is a multi-disciplinary open access archive for the deposit and dissemination of scientific research documents, whether they are published or not. The documents may come from teaching and research institutions in France or abroad, or from public or private research centers.

L'archive ouverte pluridisciplinaire **HAL**, est destinée au dépôt et à la diffusion de documents scientifiques de niveau recherche, publiés ou non, émanant des établissements d'enseignement et de recherche français ou étrangers, des laboratoires publics ou privés.

Extra modes of operation and self motions in manipulators designed for Schoenflies motion

Michel Coste* Kartoue Mady Demdah†

August 19, 2014

Abstract

We study 4-UPU parallel manipulators performing Schoenflies motion and show that they can have extra modes of operation with 3 degrees of freedom, depending on the geometric parameters of the manipulators. We show that the transition between the different modes occurs along self-motion of the manipulator in the Schoenflies mode.

Keywords: Parallel manipulators, Schoenflies motion, mode of operation, self-motion

1 Introduction

Several architectures have been proposed and studied for parallel manipulators with 4 d.o.f. (degrees of freedom) in order that they perform Schoenflies motion: 3 d.o.f. in translation and 1 d.o.f. in rotation with fixed direction of axis (in general taken to be vertical); see for instance [1-11]. Among these manipulators are 4-U$\underline{P}$U which have been proposed in [3, 7, 11]. We show in this paper that these 4-U$\underline{P}$U may also have other modes of operation, according to the geometric parameters of the architecture. The fact that parallel manipulators can have several modes of operation is well known and has been studied in the case of 3-R$\underline{P}$S in [12]. In the case of the 4-U$\underline{P}$U, the extra modes of operations, when they exist, have 3 d.o.f., that is one less than the Schoenflies mode. We also show that the transition poses between the Schoenflies mode and the extra mode are poses from which the manipulator has a circular self-motion in the Schoenflies mode.

The paper is organized as follows. We describe the manipulator under study in Section 2. We study its different modes of operation in Section 3. Then we establish in Section 4 the relationship between self-motion in the Schoenflies mode and transition poses to the extra modes of operation, when they exist. Finally we study briefly in Section 5 the influence of modification of the architecture on the existence of the extra modes of operation.

*Michel Coste: IRMAR, Université de Rennes 1, France
michel.coste@univ-rennes1.fr

†Kartoue Mady Demdah: Dep. of Mathematics, University of N'Djamena, Chad
kartoue@hotmail.com

2 The 4-UPU manipulator

The manipulator has four identical legs. The basis is a horizontal rectangle with vertices $B_1 = (a, b, 0)^{\mathbf{T}}$, $B_2 = (-a, b, 0)^{\mathbf{T}}$, $B_3 = (-a, -b, 0)^{\mathbf{T}}$, $B_4 = (a, -b, 0)^{\mathbf{T}}$. The platform is also a rectangle with vertices of coordinates $P_1 = (c, d, 0)^{\mathbf{T}}$, $P_2 = (-c, d, 0)^{\mathbf{T}}$, $P_3 = (-c, -d, 0)^{\mathbf{T}}$, $P_4 = (c, -d, 0)^{\mathbf{T}}$ in an orthonormal frame attached to the platform. We assume $a, b, c, d > 0$. The coordinates of the vertices of the platform in the fixed orthonormal frame are $Q_i = R\,P_i + T$ for $i = 1, \ldots, 4$, where R is the rotation matrix giving the orientation of the platform and T the translation vector giving the position of the centre of the platform. The vertical unit vector $V = (0, 0, 1)^{\mathbf{T}}$ is orthogonal to the base and $N = R\,V$ is a unit vector orthogonal to the platform (see Fig. 1, left).

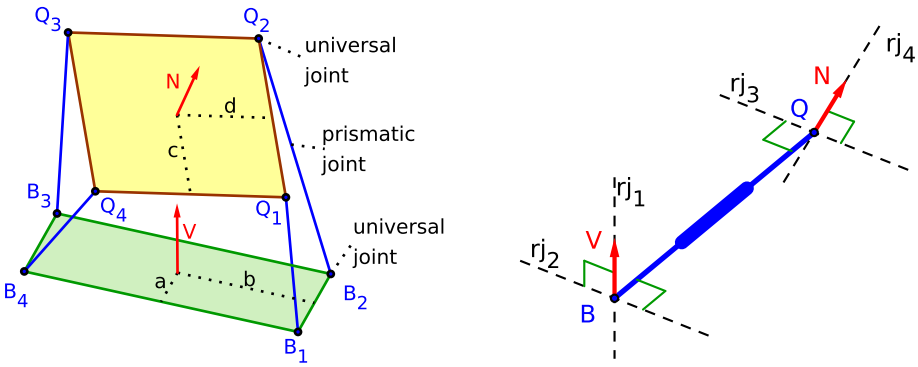

Figure 1: Left: the 4-UPU. Right: geometry of a leg; dashed lines are the axes of rotoidal joints

Each leg joining B_i to Q_i has a universal joint in B_i (decomposed in two rotoidal joints $rj_{i,1}$ and $rj_{i,2}$), a prismatic joint on the segment $[B_iQ_i]$ and another universal joint in Q_i (decomposed in two rotoidal joints $rj_{i,3}$ and $rj_{i,4}$). The axis of $rj_{i,1}$ is vertical (parallel to V), the axis of $rj_{i,4}$ is orthogonal to the platform (parallel to N) and the axes of $rj_{i,2}$ and $rj_{i,3}$ are parallel, both orthogonal to V, to N and to the vector $Q_i - B_i$ (see Fig. 1, right).

The disposition of the axes yields the constraints that $V, N, Q_i - B_i$ have to be coplanar for $i = 1, \ldots, 4$. These constraints are satisfied if $N = V$, i.e. if the manipulator stays in the *Schoenflies mode of operation* with 3 d.o.f. in translation and 1 d.o.f. in rotation, the rotations having vertical axis. The constraints are also satisfied if $N = -V$, i.e. if the platform is horizontal and upside down. This mode of operation has also 4 d.o.f. (3 in translation and 1 in rotation) and one can move from one pose in this mode to any other by a Schoenflies motion with vertical axis of rotation. So we call this mode the *reverse-Schoenflies mode of operation*.

We shall see in the next section that the constraints may also be satisfied in other modes of operation of the manipulator, depending on the architectural parameters a, b, c, d.

3 Different modes of operation

3.1 The constraint equations

In order to write down the constraint equations, we choose a rational parametrization of the group of spatial rotations, namely the Cayley parametrization:

$$R = \frac{1}{\Delta}\begin{pmatrix} 1+p^2-q^2-r^2 & 2(pq-r) & 2(rp+q) \\ 2(pq+r) & 1-p^2+q^2-r^2 & 2(qr-p) \\ 2(rp-q) & 2(qr+p) & 1-p^2-q^2+r^2 \end{pmatrix} \qquad (1)$$
$$\text{where } \Delta = 1+p^2+q^2+r^2 \ .$$

The vector $(p,q,r)^{\mathbf{T}}$ gives the oriented axis of the rotation and $\sqrt{p^2+q^2+r^2}$ is the tangent of the half-angle of rotation; the matrix R is the rotation matrix associated to the quaternion $1+ip+jq+kr$. So this parametrization misses the half-turns. In particular, we shall not obtain the poses in the reverse-Schoenflies mode of operation. This drawback is the price we pay for simple computation and output. We shall see in subsection 3.4 how to circumvent this drawback.

We set $T = (x,y,z)^{\mathbf{T}}$ for the translation vector; so we have six pose variables x,y,z,p,q,r. The constraint equations are $\det(V, N, Q_i - B_i) = 0$ for $i = 1,\dots,4$. Chasing the denominator $1+p^2+q^2+r^2$, we obtain

$$\begin{aligned} (qr-p)x-(rp+q)y+(-(b+d)r-a+c)p+((a+c)r-b+d)q &= 0 \ , \\ (qr-p)x-(rp+q)y+((b+d)r-a+c)p+((a+c)r+b-d)q &= 0 \ , \\ (qr-p)x-(rp+q)y+(-(b+d)r+a-c)p+(-(a+c)r-b+d)q &= 0 \ , \\ (qr-p)x-(rp+q)y+((b+d)r+a-c)p+(-(a+c)r+b-d)q &= 0 \ . \end{aligned} \qquad (2)$$

3.2 The components of the set of admissible poses

The four polynomials listed in the system (2) generate an ideal **Const** in the ring of polynomials in x,y,z,p,q,r with coefficients depending on the parameters a,b,c,d. Actually z does not appear in the constraint equations. The different modes of operation are studied by decomposing the ideal **Const** into primary components, as done for instance in [12]. This decomposition over the field $\mathbb{R}(a,b,c,d)$ (performed with Maple, or with Singular) gives two components $\mathbf{Const} = \mathbf{Schoenflies} \cap \mathbf{Extra}$, where

$$\begin{aligned} \mathbf{Schoenflies} &= \langle p,q \rangle \ , \\ \mathbf{Extra} &= \langle (a+c)(b+d)r^2+(a-c)(b-d), \\ &\qquad (b+d)rp+(b-d)q, \quad c(b+d)rx+d(a-c)y \rangle \ . \end{aligned} \qquad (3)$$

This decomposition means, from the geometric viewpoint, that the set of poses satisfying the constraint equations (and whose rotation part is not a half-turn) splits in two parts:

- The poses for which $p = q = 0$, i.e. the poses for which the rotation axis is vertical. These are the poses corresponding to the Schoenflies mode of operation.
- The poses satisfying the three equations generating the ideal **Extra**.

We now examine more closely the **Extra** component. The first equation in r has no real solution if $(c-a)(b-d) < 0$; in this case, there is no pose satisfying this equation and the only mode of operation is the Schoenflies mode (besides the reverse-Schoenflies mode, see below in subsection 3.4). If $(c-a)(b-d) > 0$, there are two real solutions

$$r_{\mathrm{sol}\pm} = \pm\sqrt{\frac{(c-a)(b-d)}{(a+c)(b+d)}}\,. \tag{4}$$

For each of these solutions $r_{\mathrm{sol}+}$ and $r_{\mathrm{sol}-}$, we have a mode of operation (indexed by $+$ or $-$) consisting of the poses such that

$$r = r_{\mathrm{sol}\pm}\,, \quad (d-b)\,q = (b+d) r_{\mathrm{sol}\pm}\,p\,, \quad d(c-a)\,y = c(b+d) r_{\mathrm{sol}\pm}\,x\,. \tag{5}$$

In each of these modes of operation the translation vector $(x, y, z)^{\mathbf{T}}$ ranges in a vertical plane and the rotation vector $(p, q, r)^{\mathbf{T}}$ ranges in a line. There are two d.o.f. in translation and one in rotation. Note that the symmetry w.r.t. the plane $x = 0$, or the plane $y = 0$, carries the mode of operation $+$ to $-$ and vice-versa.

It remains the case $(c-a)(b-d) = 0$. In this case there is only one extra mode of operation. In order to determine this extra mode, one has to recompute the primary decomposition in the special case since the computation giving (3) is made for generic parameters a, b, c, d.

- If $a = c$ and $b \neq d$, this mode of operation consists of the poses such that $q = r = x = 0$. There are three d.o.f.: the centre of the platform can move in the (y, z) plane, while the platform can rotate around an axis parallel to the x-axis.
- If $a \neq c$ and $b = d$, this mode of operation consists of the poses such that $p = r = y = 0$. There are three d.o.f.: the centre of the platform can move in the (x, z) plane while the platform can rotate around an axis parallel to the y-axis.
- Finally when $a = c$ and $b = d$ (congruent base and platform), the extra mode of operation consists of the poses such that $r = 0$ and $px + qy = 0$; there are four d.o.f. for this mode.

Except for the case of congruent base and platform, the extra modes of operation can be described in a unified way. Assume for instance $a \leq c$ and $b \geq d$ and set

$$\delta_1 = \sqrt{c^2 - a^2} \quad \text{and} \quad \delta_2 = \sqrt{b^2 - d^2}\,. \tag{6}$$

Then the extra modes of operation are described by:

$$r = \pm\frac{\delta_1\,\delta_2}{(a+c)(b+d)}\,, \quad \delta_2\,(a+c)\,q = \mp\delta_1\,(b+d)\,p\,, \quad \delta_1\,d\,y = \pm\delta_2\,c\,x\,. \tag{7}$$

In each of these extra modes, the axes of the rotoidal joints $rj_{i,2}$ and $rj_{i,3}$ remain parallel to the fixed vector $(\delta_2\,c, \mp\delta_1\,d, 0)^{\mathbf{T}}$.

3.3 An example

We give an example of the extra mode of operation for a manipulator with parameters $a = 1$, $b = 3$, $c = d = 2$. Then $\delta_1 = \sqrt{3}$ and $\delta_2 = \sqrt{5}$. We take $r = 1/\sqrt{15}$. We fix $x = y = 0$, $z = 5$. We let p vary from 0 to $+\infty$, keeping $q = -\sqrt{5/3}\,p$. The motion is represented in Fig. 2. It starts with a pose in the Schoenflies mode and finishes with a pose in the reverse-Schoenflies mode. The second row of Fig. 2 shows the motion from a viewpoint orthogonal to the vector $(\sqrt{5}, -\sqrt{3}, 0)^{\mathbf{T}}$. It shows that the legs remain in vertical planes orthogonal to this vector, because the axes of $rj_{i,2}$ and $rj_{i,3}$ remain parallel to this vector during the motion.

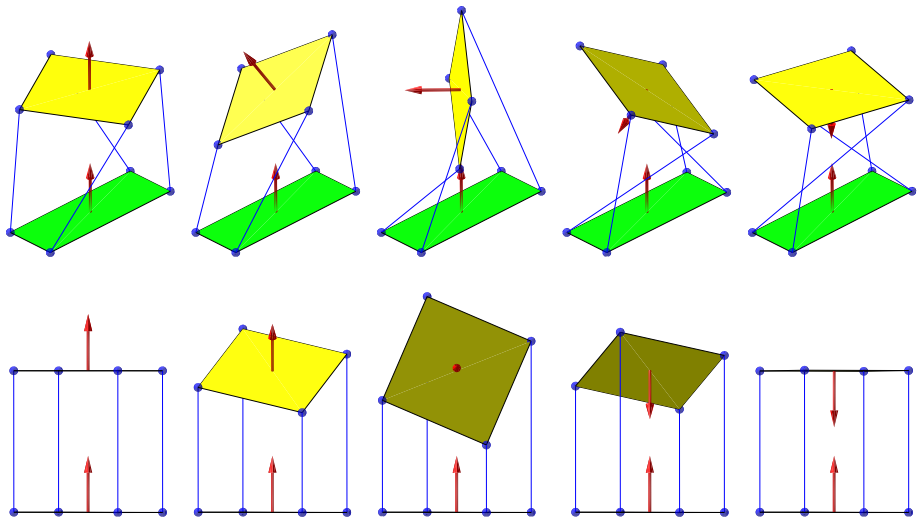

Figure 2: Motion from the Schoenflies mode to the reverse-Schoenflies mode from two different viewpoints

3.4 Recovering the half-turns

The parametrization we have chosen for the rotation group misses the half-turns. Hence, the analysis of the ideal generated by the constraint equations misses the reverse-Schoenflies mode of operation. It could be the case that it also misses other modes of operation. We check now that this is not the case.

We can change the initial pose for a pose where the platform is already upside down, for instance we can perform an initial half-turn of the platform around the x-axis. This has the effect of exchanging d and $-d$. Once this change performed, we can proceed with exactly the same analysis as before, denoting by p', q', r' the new rotation variables. The relations $p' = -1/p$, $q' = -r/p$ and $r' = q/p$ between the two sets of rotation variables are obtained by writing that the quaternion $(1 + ip' + jq' + kr')\,i$ is a real multiple of $1 + ip + jq + kr$.

The primary decomposition of the ideal generated by the constraint equations in the variables x, y, z, p', q', r' is obtained from (3) by exchanging d with

$-d$. It gives the two components

$$\begin{aligned}\mathbf{RevSchoenflies} &= \langle p', q' \rangle \ , \\ \mathbf{Extra}' &= \langle (a+c)(b-d)r'^2 + (a-c)(b+d), \\ &\qquad (b-d)r'p' + (b+d)q', \quad c(b-d)r'x - d(a-c)y \rangle \ .\end{aligned} \tag{8}$$

The first equation in r' of the $\mathbf{Extra}'$ component has real solutions if and only if $(c-a)(b-d) \geq 0$, and the solutions in r' then give the extra modes of operation already identified.

We can also repeat the same analysis starting now with an initial half-turn around the y-axis, which amounts to exchanging c and $-c$. We have then recovered all half-turns, except the one around the z-axis which belongs to the Schoenflies mode. The analysis of the modes of operation is indeed complete.

We could also have used the parametrization of the rotation group using unit quaternions. The computation of the primary decomposition of the ideal generated by the constraint equations is then more difficult, but can still be performed with Singular; it gives three components corresponding to the Schoenflies mode, the reverse-Schoenflies mode, and the possible extra modes. Also, the output of this computation is less easily readable for the extra component. However, it confirms the results explained in this section.

4 Self-motions and transition between the modes

4.1 Poses of transition from the Schoenflies mode to an extra mode

In this section we shall always consider the manipulator in Schoenflies mode of operation. The rotation matrix is here restricted to have a vertical axis, so we can write it as

$$R = \begin{pmatrix} \cos(\theta) & -\sin(\theta) & 0 \\ \sin(\theta) & \cos(\theta) & 0 \\ 0 & 0 & 1 \end{pmatrix} \tag{9}$$

The pose variables for the Schoenflies mode are θ, x, y, z. Comparing with the (p, q, r) orientation variables of the preceding section, we have here $p = q = 0$ and $r = \tan(\theta/2)$.

We also restrict our attention to the case $(c-a)(b-d) > 0$ where there are two extra modes of operation with 3 d.o.f. besides the Schoenflies and reverse-Schoenflies modes. We assume $a < c$ and $b > d$, so that we can use the quantities $\delta_1 = \sqrt{c^2 - a^2}$ and $\delta_2 = \sqrt{b^2 - c^2}$. According to the analysis of the preceding section, each extra mode (denoted with $+$ or $-$) intersects the Schoenflies mode in the set of poses which satisfy

$$\theta = \pm \arccos\left(\frac{ab+cd}{ad+bc}\right), \quad \delta_1 \, d \, y = \pm \delta_2 \, c \, x \ . \tag{10}$$

These transition poses form two vertical planes $\mathbf{TR}_\pm$ (of dimension 2). We shall now compare the transition poses with actuation singularities in the Schoenflies mode.

4.2 Actuation singularities in the Schoenflies mode

The actuated joints are the four prismatic joints on the legs. We use as coordinates in the joint space $\rho_i = \|Q_i - B_i\|^2$, the squares of the lengths of the legs, for $i = 1, \ldots, 4$. The inverse kinematic mapping for the Schoenflies mode is $(\theta, x, y, z) \mapsto (\rho_1, \rho_2, \rho_3, \rho_4)$. The Jacobian determinant of the inverse kinematic mapping is, up to a constant factor (cf [13, (4.97)] or [11]):

$$J = (ad - bc)\, \cos(\theta)\, ((ad + bc)\cos(\theta) - (ab + cd))\, z\ . \tag{11}$$

The structure of the inverse kinematic mapping and its singularities are more easily understood after a linear change of coordinates in the joint space. Set

$$\sigma_1 = (\rho_1 - \rho_2 + \rho_3 - \rho_4)/8,\ \sigma_2 = (\rho_1 - \rho_3)/4,\ \sigma_3 = (\rho_2 - \rho_4)/4,\ \sigma_4 = \rho_4\ . \tag{12}$$

Then the inverse kinematic mapping is rewritten as

$$\begin{aligned}
\sigma_1 &= \sin(\theta)\,(ad - bc)\ ,\\
\sigma_2 &= (\cos(\theta)\,c - \sin(\theta)\,d - a)\,x + (\sin(\theta)\,c + \cos(\theta)\,d - b)\,y\ ,\\
\sigma_3 &= (-\cos(\theta)\,c - \sin(\theta)\,d + a)\,x + (-\sin(\theta)\,c + \cos(\theta)\,d - b)\,y\ ,\\
\sigma_4 &= (x + \cos(\theta)\,c + \sin(\theta)\,d - a)^2 + (y + \sin(\theta)\,c - \cos(\theta)\,d + b)^2 + z^2\ ,
\end{aligned} \tag{13}$$

which shows that σ_1 depends only on θ and σ_2 and σ_3 depend linearly on x, y with coefficients depending on θ. The factor $(ad-bc)\,\cos(\theta)$ of J is the derivative of σ_1 w.r.t. θ, the factor $(ad + bc)\cos(\theta) - (ab + cd)$ is the determinant of the linear mapping $(x, y) \mapsto (\sigma_2, \sigma_3)$ and the factor z is half of the derivative of σ_4 w.r.t. z. We shall assume in what follows that $ad - bc \neq 0$, i.e. that the base and the platform are not similar (in this case the manipulator is completely singular and there is self-motion from every pose).

We concentrate our attention on the actuation singularities satisfying the equation $(ad + bc)\cos(\theta) = ab + cd$. This equation has two solutions precisely when $(c - a)(b - d) > 0$, and the solutions in θ are

$$\theta_{\mathrm{sol}\pm} = \pm \arccos\left(\frac{ab + cd}{ad + bc}\right)\ . \tag{14}$$

The poses satisfying $\theta = \theta_{\mathrm{sol}\pm}$ form two components $\mathbf{AS}_\pm$ (which are spaces of dimension 3) of the actuation singularities of the Schoenflies mode. We are interested in these components of the actuation singularities because, according to (10), each component $\mathbf{AS}_\pm$ contain a plane $\mathbf{TR}_\pm$ of intersection with an extra mode.

4.3 Self-motion in the Schoenflies mode

The image of a component $\mathbf{AS}_\pm$ of the actuation singularities in the joint space is contained in a plane $\mathbf{P}_\pm$. Indeed we have

$$\sin(\theta_{\mathrm{sol}\pm}) = \pm\frac{\delta_1\,\delta_2}{ad + bc} \tag{15}$$

so that setting $\theta = \theta_{\mathrm{sol}\pm}$ in (13) yields

$$\begin{aligned}
\sigma_1 &= \pm(ad-bc)\,\frac{\delta_1\,\delta_2}{ad+bc}\ ,\\
\sigma_2 &= \frac{\delta_1 \mp \delta_2}{ad+bc}\,(d\,\delta_1\,x \pm c\,\delta_2\,y)\ , \quad \sigma_3 = \frac{\delta_1 \pm \delta_2}{ad+bc}\,(-d\,\delta_1\,x \mp c\,\delta_2\,y)\ ,\\
\sigma_4 &= \left(x - \frac{d\,\delta_1\,(-\delta_1 \mp \delta_2)}{ad+bc}\right)^2 + \left(y - \frac{c\,\delta_2\,(\mp\delta_1 - \delta_2)}{ad+bc}\right)^2 + z^2\ .
\end{aligned} \tag{16}$$

This shows that the image of $\mathbf{AS}_\pm$ is contained in the plane $\mathbf{P}_\pm$ defined by the equations

$$\sigma_1 = \pm(ad-bc)\,\frac{\delta_1\,\delta_2}{ad+bc} \quad \text{and} \quad (\delta_1 \pm \delta_2)\,\sigma_2 + (\delta_1 \mp \delta_2)\,\sigma_3 = 0 \tag{17}$$

Since $\mathbf{AS}_\pm$ is of dimension 3 and its image in the joint space is of dimension 2, there is self-motion from almost every pose in $\mathbf{AS}_\pm$. The equations (16) of the inverse kinematic mapping restricted to $\mathbf{AS}_\pm$ give the information about this self-motion: it occurs along the vertical circle $\mathbf{\Gamma}_\pm$ which is the intersection of the vertical plane $\mathbf{\Pi}_\pm$ given by the second or third equation of (16) and the sphere $\mathbf{\Sigma}_\pm$ given by the fourth equation. This intersection is reduced to a point for $(\sigma_1, \sigma_2, \sigma_3, \sigma_4)$ belonging to a parabola in the plane $\mathbf{P}_\pm$, and it is empty outside of the parabola; the equation of the parabola is obtained by writing that the square of the distance of the center of $\mathbf{\Sigma}_\pm$ to $\mathbf{\Pi}_\pm$ (a quadratic expression in σ_2 or σ_3) is equal to the square of the radius of $\mathbf{\Sigma}_\pm$, which is σ_4.

Observe that the vertical plane $\mathbf{TR}_\pm$ (equation $\pm\delta_2\,c\,x - \delta_1\,d\,y = 0$) is perpendicular to the vertical plane $\mathbf{\Pi}_\pm$ (second or third equation of (16)). Observe also that the center of the sphere $\mathbf{\Sigma}_\pm$ of coordinates

$$\left(\frac{d\,\delta_1\,(-\delta_1 \mp \delta_2)}{ad+bc},\ \frac{c\,\delta_2\,(\mp\delta_1 - \delta_2)}{ad+bc},\ 0\right)$$

belongs to $\mathbf{TR}_\pm$. It follows that each circle $\mathbf{\Gamma}_\pm$ of self-motion (intersection of $\mathbf{\Sigma}_\pm$ with $\mathbf{\Pi}_\pm$) contains two poses which allow transition to the extra $\pm$ mode; these poses are those with maximal and minimal values of z on the circle. The transition between modes of operation in self-motions was already observed for 3-RPS in [14]. See Fig. 3 which shows the geometry of the objects mentioned above in an example.

4.4 Example continued

We give an example of self-motion in the Schoenflies mode for the same manipulator as the one in Fig. 2. The self-motion from the pose $x = y = 0$, $z = 5$, $\theta = \arccos(7/8)$, which is a transition pose to an extra mode, is shown in Fig. 4. The picture on the right shows the self-motion from a viewpoint in the direction of the vector $(\sqrt{3}, \sqrt{5}, 0)^{\mathbf{T}}$ (as in the second row of Fig. 2); the legs are always in parallel planes and a transition pose is attained when these planes are vertical. Note that the direction of the vertical planes of self-motion is perpendicular to the direction of the vertical planes of motion in the extra mode.

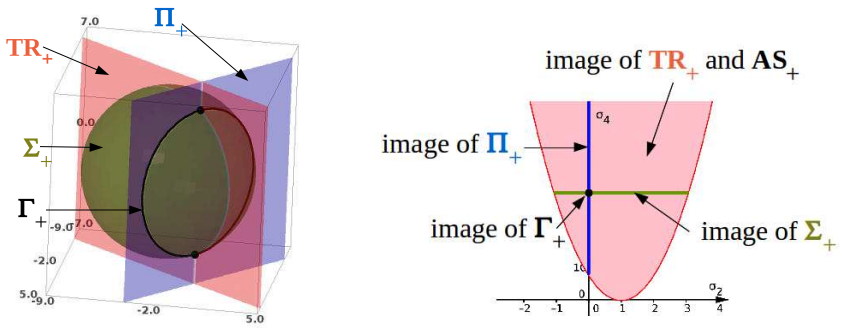

Figure 3: Left: picture of $\mathbf{AS}_+$, 3-d component of actuation singularities in the workspace. Right: Picture of $\mathbf{P}_+$, plane in in the joint space containing the image of $\mathbf{AS}_+$ under IKM

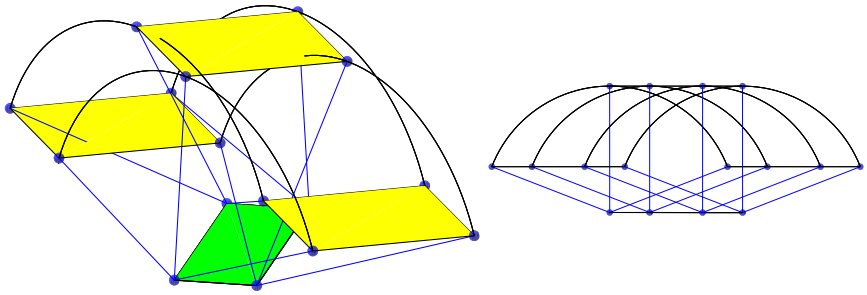

Figure 4: Two viewpoints on self-motion along vertical circle in the Schoenflies mode. The top pose is a transition to an extra mode of operation

5 Variants in the architecture

5.1 Rhombus base and platform

The case when the base and the platform are rhombi instead of rectangles (as in [11]) can be dealt with in exactly the same way. Taking $B_1 = (a, 0, 0)^{\mathbf{T}}$, $B_2 = (0, b, 0)^{\mathbf{T}}$, $B_3 = (-a, 0, 0)^{\mathbf{T}}$, $B_4 = (0, -b, 0)^{\mathbf{T}}$, $P_1 = (c, 0, 0)^{\mathbf{T}}$, $P_2 = (0, d, 0)^{\mathbf{T}}$, $P_3 = (-c, 0, 0)^{\mathbf{T}}$, $P_4 = (0, -d, 0)^{\mathbf{T}}$ leads to the same condition $(c-a)(b-d) \geq 0$ for the existence of extra operation modes. We shall not comment further this case

5.2 Moving one anchor point

The reason for the existence of extra modes of operations lies in the fact that one can rotate the platform rectangle in such a way that the corresponding vertices of the base and the platform lie on parallel lines (see Fig. 5). If the condition $(c-a)(b-d) > 0$, there are two opposite angles of rotation θ given by formula (10) leading to this situation. Figure 5 represents the two rotations in the case of the example $a = 1$, $b = 3$, $c = d = 2$; The rotation leading to the operation

mode labelled + (resp. −) is represented in blue (resp. brown).

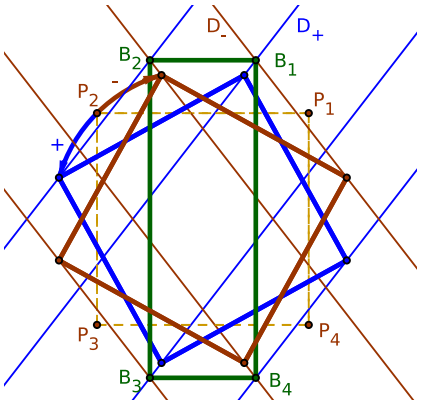

Figure 5: Rotations of the platform explaining the extra modes of operation

If one moves an anchor point on the base (B_1, for instance) along the line D_+ (see Fig. 5), then the extra mode of operation labelled + persists, but the mode labelled − disappears; the same happens for D_-, exchanging + and −. If B_1 is moved out of the union of the two lines D_+ and D_-, both extra modes of operation disappear. This shows that the existence of these extra modes of operation is a non generic situation which does not occur if the base and platform are general quadrilaterals.

6 Conclusion

We have studied a 4-UPU manipulator which is designed to perform Schoenflies motion. We have shown that, besides the Schoenflies and reverse Schoenflies (upside down) modes of operation with 4 d.o.f., this manipulator can offer two extra modes of operation with 3 d.o.f.. We have characterized the manipulators which have this property in terms of the dimensions a, b of the base rectangle and c, d of the platform rectangle: a necessary and sufficient condition is $((c - a)(b - d) > 0$.

We have studied the poses in the Schoenflies mode for which there is a transition to an extra mode, when this condition is satisfied. We have shown that these transition poses belong to components of the actuation singularities. The manipulator has self-motion along vertical circles on these components, and on each circle of self-motion there are two transition poses. We have also shown that the existence of these extra modes of operation is a non generic situation, which disappears for small general modifications of the architecture.

References

[1] L. Rolland: *The Manta and the Kanuk: Noved 4 dof parallel mechanism for industrial handling.* In *Proc. of ASME Dynamic Systems and Control*

Division IMECE'99 Conference, Nashville, USA, November 14-19, 1999, vol. 67, pp. 831-844.

[2] F. Pierrot and O. Company: *H4: a new family of 4-dof parallel robots*. In *Proc. of the IEEE/ASME Int. Conf. on Advanced Intelligent Mechatronics*, Atlanta, USA, 1999, pp. 508-513.

[3] T.S. Zhiao, J.S. Dai and Z. Huang: *Geometric Analysis of Overconstrained Parallel Manipulators with Three and Four Degrees of Freedom*. JSME International Journal C **45** (2002), 730-740

[4] O. Company, F. Marquet and F. Pierrot F.: *A new high speed 4-dof parallel robot. Synthesis and modeling issues*. IEEE Trans. on Robotics and Automation **19** (2003), 411-420

[5] X. Kong and C.M. Gosselin: *Type synthesis of 3T1R 4-dof parallel manipulators based on screw theory*. IEEE Trans. on Robotics and Automation **20** (2004), 181-190

[6] Q-C. Li and Z. Huang: *Mobility analysis of a novel 3-5R parallel mechanism family*. ASME J. of Mechanical Design **126** (2004), 79-82

[7] T.S. Zhao, Y.W. Li, J. Chen and J.C. Wang: *Novel Four-DOF Parallel Manipulator Mechanism and Its Kinematics*. In *Robotics, Automation and Mechatronics, 2006 IEEE Conference*. D.O.I. 10.1109/RAMECH.2006.252672

[8] G. Gogu: *Structural synthesis of fully isotropic parallel robots with Schoenflies motions via theory of linear transformations and evolutionary morphology*, European Journal of Mechanics A/ Solids, **26** (2007), 242-269

[9] S. Amine, S. Caro, P. Wenger and D. Kanaan: *Singularity Analysis of the H4 Robot using Grassmann-Cayley Algebra*, Robotica **30** (2012), 1109-1118

[10] S. Amine, M. Tale-Masouleh, S. Caro, P. Wenger and C. Gosselin: *Singularity Conditions of 3T1R Parallel Manipulators with Identical Limb Structures*, ASME Journal of Mechanisms and Robotics, **4** (2012) 011011-1-011011-11

[11] M. Solazzi, M. Gabardi, A. Frisoli, and M. Bergamasco: *Kinematics analysis and singularity loci of a 4-UPU parallel manipulator*. In J. Lenarçic and O. Khatib, eds: *Advances in Robot Kinematics 2014*, pp. 467-474. Springer, 2014.

[12] J. Schadlbauer, D.R. Walter, M.L. Husty: *The 3-RPS parallel manipulator from an algebraic viewpoint*, Mechanism and Machine Theory 75 (2014), 161-176

[13] J. Zhao, Z. Feng, F. Chu, N. Ma: *Advanced Theory of Constraint and Motion Analysis for Robot Mechanisms*. Academic Press, 2013

[14] M.L. Husty, J. Schadlbauer, S. Caro and P. Wenger: *Self-motions of 3-RPS manipulators*. In F. Viadero, M. Ceccarelli (Eds.): *New Trends in Mechanism and Machine Science, Theory and Application in Engineering, Mechanism and Machine Science*, 7, Springer-Verlag, 2012, pp. 121-130.